Refinement of Low Resolution DEM Using Differential Interferometry

Chang-Oh Kim, Dong-Cheon Lee, Jeong-Woo Kim
Dept. of Geoinformation Engineering, Sejong University
98 Gunja-Dong Gwangin-Gu, Seoul 143-747, Korea
bonking@hanmail.net

Sang-Wan Kim, Joong-Sun Won
Dept. of Earth System Sciences, Yonsei University
134 Shinchon-Dong, Seodaemun-Gu, Seoul 120-749, Korea

Abstract: Interferometry SAR (InSAR) is a technique to generate topographic map from complex data pairs observed by antennas at different locations. However, to obtain topographic information using InSAR is difficult task because it requires series of complicated process including phase unwrapping and precise recovery of the SAR geometry. Especially, accuracy of the DEM (Digital Elevation Model) produced by repeat pass single SAR pair could be influenced by atmospheric effect. Recently, a new InSAR technique to improve accuracy of DEM has been introduced that utilizes low resolution DEM with a number of SAR image pairs. The coarse DEM plays an important role in reducing phase unwrapping error caused by layover and satellite orbit error. In this study, we implemented DInSAR (Differential InSAR) method which combines low resolution DEMs and ERS tandem pair images. GTOPO30 DEM with 1km resolution, SRTM-3 DEM with 100m resolution, and DEM with 10m resolution derived from 1:25,000 digital vector map were used to investigate feasibility of DInSAR. The accuracy of the DEMs generated both by InSAR and DInSAR was evaluated.

Keywords: InSAR, DInSAR, DEM, Digital vector map, Accuracy analysis.

1. Introduction

One of the main issues in SAR data processing is focused on improving DEM generated by interferometric information. InSAR uses multiple SAR data to obtain phase difference which is basis of creating topographic information including 3-dimensitonal positioning and surface displacement. DInSAR utilizes both multiple SAR data and geospatial information to generate accurate DEM. The basic concept of DInSAR is to separate phase of surface displacement effect from phase of topography effect in the interferogram. This is possible if DEM is available because DEM provides topographic information about Earth surface.

A study on DEM extraction using InSAR with SIR-B data was carried out by Gabriel and Goldstein (1988). Rufino et al. (1998) generated DEM with ERS-1/2 tandem SAR data. The methods of improving accuracy of the DEM include: (1) Elimination of areas that show low signal to noise ratio or low coherence in the process of phase unwrapping (Fazio et al., 1993), (2) Utilizing baseline information and DEM instead of ground control points (Seymour, 1999), (3) Use of SPOT stereo imagery in the areas where causes significant errors due to layover, shadow or temporal decorrelation (Honikel, 1998).

2-pass DInSAR utilizes two SAR data and DEM. One of the advantages of DInSAR is phase unwrapping is not required. The results of DInSAR depend mainly on quality of the DEM (Rosen et al., 1996). However, high quality DEM is not always available. In case of using low accuracy DEM, errors of the DEM have to be corrected to improve resulting DEM generated DInSAR. The errors could be identified in the residual phase.

This study uses ERS-1/2 tandem pair and various DEMs including GTOPO30, SRTM-3, and DEM derived from digital vector map. DEMs were generated by InSAR, and DInSAR with different initial DEMs. Finally, the accuracy of resulting DEMs was analyzed with GCPs.

2. Study Area and Description of Data

The data used in this study are ERS-1/2 tandem pair of Daejon area in Korea. Image of ERS-1 was acquired on 22 Jan. 1996 (Fig. 1(a)) and image of ERS-2 was acquired on 23 Jan. 1996 (Fig. 1(b)). The images were used for master and slave images in the respective order.

SAR data were processed by *GeoRadar* developed by Remote Sensing Laboratory/Department of Earth System Sciences in Yonsei University. Fig. 1(c) shows the post-filtered interferogram, and Fig. 1(d) shows an image of unwrapped phase.

DEMs used in the 2-pass DInSAR are 1km resolution GTOPO 30 DEM, 100m resolution SRTM-3 DEM collected by space shuttle Endeavor, and 10m resolution DEM derived from 1:25,000 digital vector Map. Total 15 GCPs obtained by GPS surveying were used to evaluate accuracy of the DEMs.

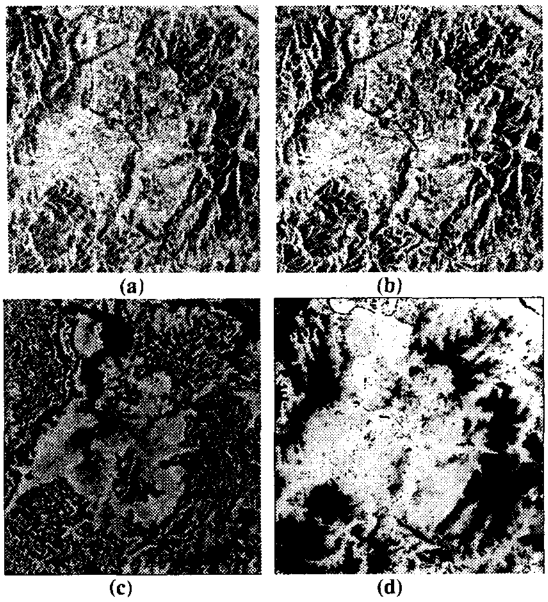

Fig.1 ERS image. (a)ERS-1 master image, (b)ERS-2 slave image, (c)filtering interferogram, (d)Unwrapped phase image.

3. Data Processing and Results

3.1 Data Processing

InSAR geometry is depicted in Fig. 2(a). The distance between the master and the slave satellite is baseline (B). The perpendicular baseline is B_p and the horizontal baseline is B_{II}. The distance between the reference surface and the satellite is H, Height of the surface from the reference surface is Z. Phase difference and elevation are computed by equation (1) and (2), respectively.

$$\Delta\phi = 2(R_2 - R_1)\frac{2\pi}{\lambda} \qquad (1)$$

$$Z = H - R_1 \cos\theta_1 \qquad (2)$$

Fig. 2(b) of phase difference are computed by equation (3),

$$\phi = -(4\pi / \lambda)\delta\rho \qquad (3)$$

Fig. 3(a) describes steps of the InSAR processing. The first step of InSAR processing is to generate SLC (Single Look Complex) data from raw data, then image co-registration is followed. Interferogram is produced by calculating coherence. The generated interferogram which contains phase effect introduced by curvature of the Earth was adjusted. In the phase unwrapping stage, the fact that phase is relevant to the relief of the Earth surface has to be considered. Lastly, conversion to height is to be performed to generate DEM.

On the other hand, DInSAR uses both SLC data and DEM, then quality of the initial DEM is eventually improved (Fig. 3(b)). Phase effect due to displacement of the Earth surface during data acquisition is ignored since ERS-1/2 tandem data were used. Therefore, if the resulting DEM and the input DEMs to the DInSAR are accurate, there is not surface displacement theoretically. In such case, therefore, fringes in the interferogram represent presence of the elevation error of the DEM only. In addition, satellite PRF (Pulse Recurrence Frequency) and orbit information are required to generate DEM.

A phase unwrapping method introduced by Flynn(1997) was implemented. Flynn's method is more efficient than the brance cut method introduced by Goldstein et al.(1988) and the minimum L^P-norm method (Kim, et al., 2000).

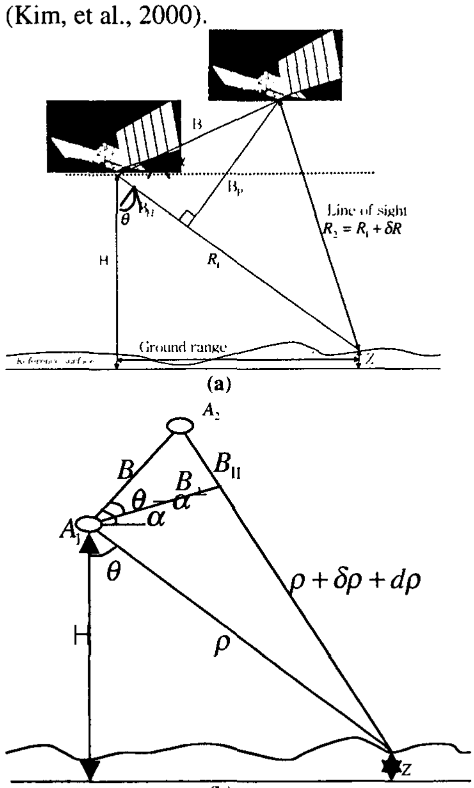

Fig.2 Radar Geometry (a)Imaging Geometry for InSAR, (b)Imaging geometry for DInSAR

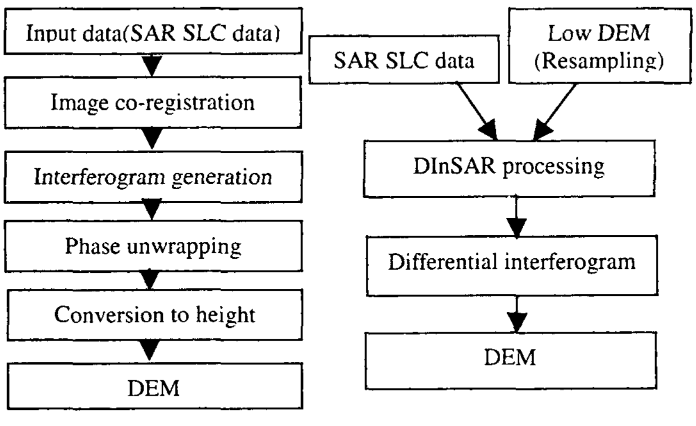

Fig.3 Data Processing. (a)InSAR, (b)DInSAR

3.2 Results and Analysis

The DEM generated on WGS84 ellipsoid and UTM system (Fig.4). Since SAR imagers refer radar coordinate system, GCPs were used as reference points for coordinate transformation between radar and UTM systems. Orthoimage is created for each DEM (Fig. 5) to identify GCPs. In orthoimages, layover introduced distortion in the areas with steep slope. In order to reduce such distortion, the pixels were enlarged to various sizes for orthoimage generation. Layover occurs where the surface slope angle is larger than radar looking angle. Therefore, the radar signal at the top of the slope arrives before the signal from the bottom of the slope, causing an upside down image. Since ERS imagery has an looking angle of 23°, layovers in the mountainous areas are frequent.

Fig. 6 shows the location of GCPs. Results show that accuracy (in terms of RMSE) of GTOPO30 DEM was improved from 30.30m to 5.47m, and accuracy of DEM derived from 1:25,000 digital vector map was improved from 21.97m to 5.92m. On the other hand, accuracy of SRTM-3 DEM was not improved (Initial accuracy was 4.97m and resulting accuracy was 5.60m). However, resulting accuracy of all DEMs is almost the same. Fig. 7 and Table 1. show RMSE ranges of North- and East-coordinate, and height at GCPs.

The accuracy evaluation in the mountainous areas could not be possible because GCPs are not available in the areas. Therefore, indirect analyses of the accuracy were performed by comparing between DEMs. DEM derived from 1:25,000 digital vector map was used as the reference then height differences between DEMs were computed. The results reveal that GTOPO30 DEM and InSAR DEM have relatively larger error than SRTM-3 DEM in mountainous regions (Fig. 8).

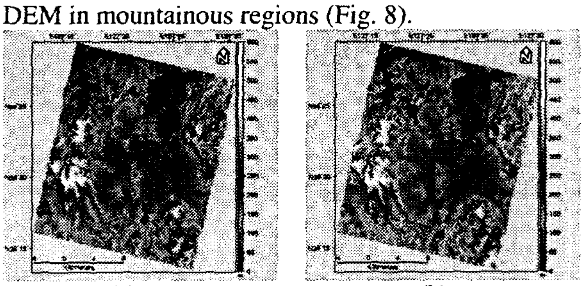

(a) (b)

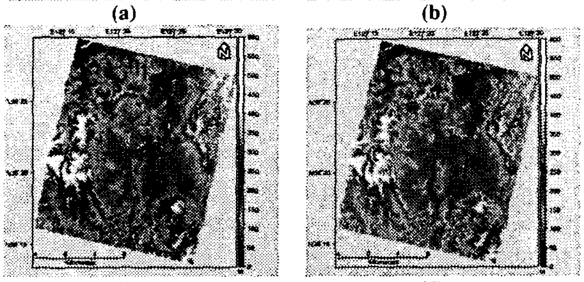

(c) (d)

Fig. 4 DEM Generation. (a)InSAR (b) DInSAR_GTOPO30 (c) DInSAR_SRTM (d) DInSAR_Digital map(1:25,000)

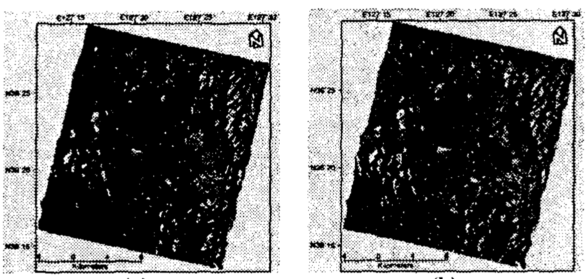

(a) (b)

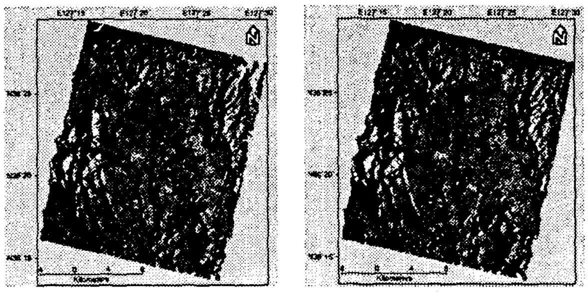

(c) (d)

Fig. 5 Ortho-image. (a)InSAR (b) DInSAR_GTOPO30 (c) DInSAR_SRTM (d) DInSAR_Digital map(1:25,000)

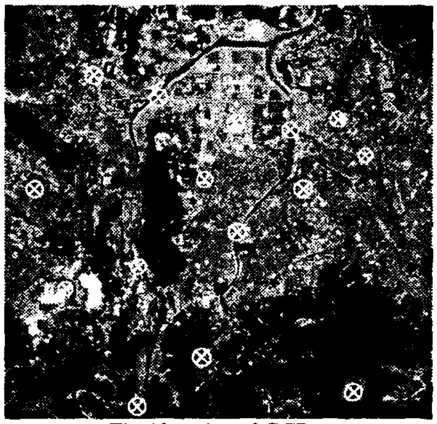

Fig.6 location of GCPs

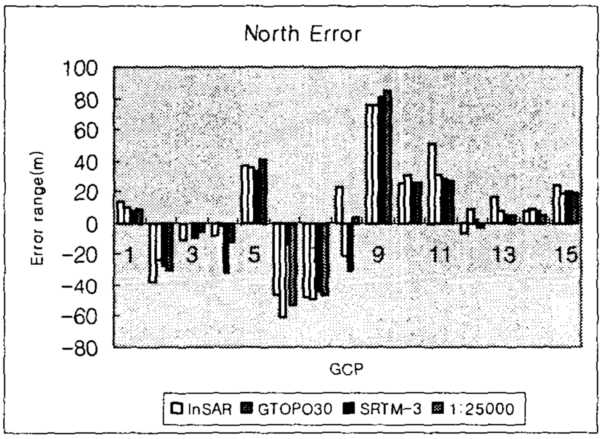

(a)

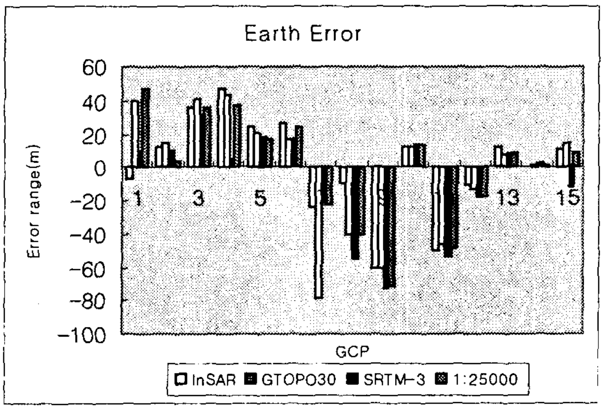

(b)

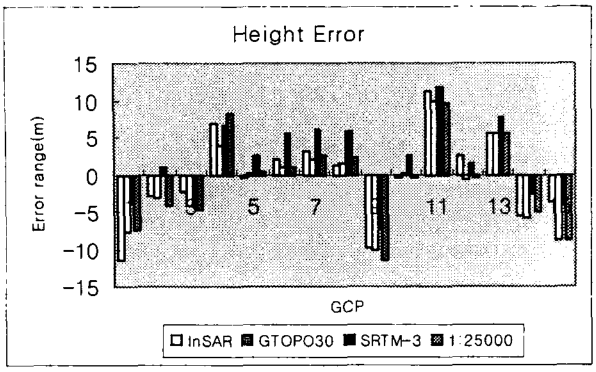

(c)

Fig.7 Error Ranges. (a) North coordinate error, (b) East coordinate Error, (c) Height Error

Table 1. RMSE (Unit:m)

	North Error	East Error	Before Height error	After Height Error
InSAR	34.77	28.74	5.86	X
DInSAR_GTOPO30	33.28	36.73	30.30	5.47
DInSAR_SRTM	30.83	30.61	4.97	5.60
DInSAR_Digital map(1:25,000)	33.34	32.82	21.97	5.92

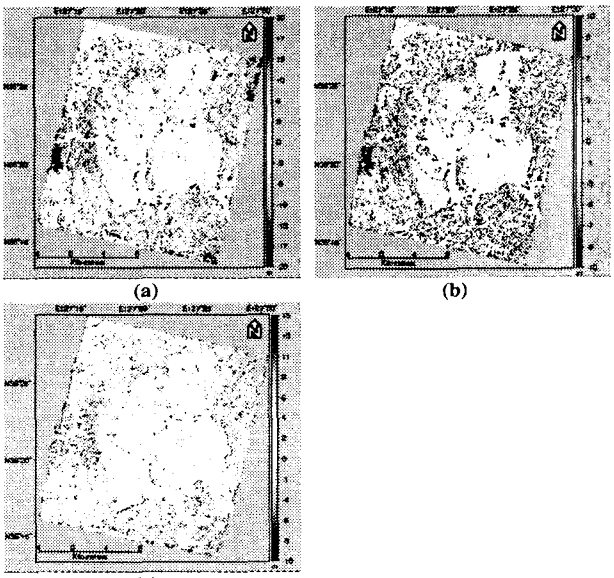

(a) (b) (c)

Fig.8 DEM Relative error calculated through digital map.
(a) DInSAR_Digital map(1:25,000)과 InSAR image
(b) DInSAR_Digital map(1:25,000)과 InSAR_GTOPO30
(c) DInSAR_Digital map(1:25,000)과 DInSAR_SRTM

4. Concluding Remarks

This paper focuses on improvement of the accuracy of DEMs by 2-pass DInSAR. Because ERS-1/2 tandem pair have an incidence angle of 23°, steep sloped areas are affected by layover. Moreover, GCPs are not available in the mountainous areas. In consequence, accuracy evaluation of DEMs may have limitation in this study.

In summary,

1. Accuracy of the DEMs was improved by implementing DInSAR.
2. The comparison between DEMs reveals that DInSAR provides more accurate DEM than InSAR especially in the mountainous areas.
3. Change detection and topographic map updating could be accomplished effectively by applying DInSAR technique.

Acknowledgement

This study was supported by the National Research Lab Project (Grant No. M1-0302-00-0063) of Korea Ministry of Science and Technology.

References

[1] Kim, S.W., Lee, H. J., and Won, J.S., 2000. SAR Interferometry Phase Unwrapping comparative analysis: using Branch cut, Minimum discontinuity, and Minimum L^P norm., The Korean Society of Remote Sensing Spring Seminar Collection 3: 96-101.

[2] Yoon, K.W., Kim, S.W., Min, K.D., Won, J.S., 2001. Application of 2-pass DInSAR to improve DEM precision. The Korean Society of Remote Sensing. 17(3): 231-242.

[3] Gabriel, A. K., and Goldstein, 1988. Crossed orbit interferometry:theory and experimental results from SIR-B, Int. J. of Remote sens., 9(5): 857-872.

[4] Goldstein R.M., Zebker H.A., and Werner C.L, 1988. Satellite radar interferometry: two-dimensional phase unwrapping. Radio Sci., 23: 713-720.

[5] Fazio, M. D., F., Vinelli, 1993. DEM reconstruction in SAR Interferometry: Practical experiences with ERS-1 SAR data, Geoscience and Remote Sensing Symposium,IGARSS '93. Better Understanding of Earth Environment., International, 3: 1207-1209.

[6] Rosen P. A., S. Hensley, H. A. Zebker, F. H. Webb, and E.J. Fielding, 1996. Surface deformation and coherence measurements of Kilauea Volcano, Hawaii, from SIR-C radar interferometry, Journal of Geophysical Research, 101(E01): 23109- 23125.

[7] Flynn, T. J, 1997. Two-dimensional Phase Unwrapping with minimum weighted discontinuity, J. Opt. Soc. Am., 14(10): 2692-2701.

[8] Honikel, M, 1998. Improvement of InSAR DEM Accuracy Using Data and Sensor Fusion, Geoscience and Remote Sensing Symposium Proceedings, IGARSS '98. 1998 IEEE International, 5: 2348-2350.

[9] Rufino G., A. Moccia, S. Esposito, 1998. DEM Generation by Means of ERS Tandem Data, IEEE Transactions on Geoscience and Remote sensding, 36(6): 1905-1912.

[10] Seymour M. S, 1999. Refining Low-quality Digital Elevation Models Using Synthetic Aperture Radar Interferometry,Doctoral thesis, the University of British Columbia.